ELSEVIER

Thermochimica Acta 293 (1997) 77–85

thermochimica acta

In vitro human skin barrier perturbation by oleic acid: Thermal analysis and freeze fracture electron microscopy studies

Hanafi Tanojo, Anita Bos-van Geest, Joke A. Bouwstra, Hans E. Junginger*, Harry E. Boddé

Division Pharmaceutical Technology, Leiden Amsterdam Center for Drug Research, Leiden University, P.O. Box 9502, 2300 RA Leiden, The Netherlands

Received 12 July 1996; accepted 12 December 1996

Abstract

This study aims to elucidate the working mechanism of oleic acid (OA) on isolated human stratum corneum (SC) sheets using two in vitro techniques, differential thermal analysis and freeze-fracture electron microscopy. Differential thermal analysis on SC after the application of OA in propylene glycol revealed significant changes in the thermal profiles of SC compared to that of the untreated SC. The changes occurred generally on the lipid phase transitions by both shifting the temperatures to a lower degree and reducing the enthalpies of the transitions normally observed between 40° and 90°C. Another newly observed change took place in the temperature range below 0°C, referred to as the subzero region. The subzero transition of OA has profoundly influenced the subzero SC lipid transition (normally observed at around −10°C) by shifting it to a lower temperature. The interesting observation was that the subzero transition of SC lipid and of OA became a single transition after the SC is heated to 120°C, which indicates a close interaction between oleic acid and SC lipids. Electron micrographs obtained by freeze-fracture electron microscopy revealed the formation of a new structure in the intercellular lipid regions of SC in the presence of OA. These findings may prove that oleic acid acts as a skin penetration enhancer by forming together with SC lipid a new type of lipid domain which are responsible for the decreased capacity of skin barrier function after oleic acid treatment. © 1997 Elsevier Science B.V.

Keywords: Differential thermal analysis; Freeze-fracture electron microscopy; Skin perturbation; Oleic acid; Propylene glycol

1. Introduction

The skin provides a good barrier for our body against penetration of most substances from outside. The main barrier of skin has been identified to be located in the uppermost layer, the stratum corneum (SC) [1,2]. For many exogenous substances, it is difficult to penetrate across the SC and reach the blood circulation system. Their penetration however can be improved and made controllable using so-called skin permeation enhancers.

The capacity of oleic acid (OA) as a skin penetration enhancer has been generally recognized [3,4]. Yet, to date the mode of action is still under deep investigation. It has been suggested that penetration enhancement can be achieved by increasing drug solubility in vehicle as well as increasing the skin penetration of the vehicle [5], by disrupting the inter-

*Corresponding author. Tel: +31-71-5274308, 0031-071-5274207; fax: +31-71-5274565, 0031-071-5274565; e-mail: junginge@chem.leidenuniv.nl.

PII S0040-6031(97)00063-4

cellular lipids and/or intracellular proteins [6], by fluidization of the skin lipid structure [7,8], or, in more recent observations, by forming separate domains which break up the continuity of the multilamellar structure and may hence induce highly permeable pathways in these domains [9–12].

In order to get a more detailed insight in the mechanism we have performed in vitro experiments on human SC pre-treated with OA, using two techniques, i.e. Differential Thermal Analysis (DTA) and Freeze-Fracture Electron Microscopy (FFEM). DTA has been used to study SC either related to bound water [13–15], or to lipid and protein thermal transitions [16–20], as well as to understand the mode of action of some enhancers on SC, such as dimethyl sulphoxide [21], azones [21–24], terpenes [25,26], surfactants [6,27], and other compounds [6]. There are five major transitions generally recognized from human SC. The temperature of these transitions and their explanations are summarized in Table 1.

Electron microscopy is a versatile tool to visualize the microstructures including those of the skin. In combination with freeze-fracture replication [28,29], this technique is able to reveal unique en face views of intramembraneous or multilamellar lipid structure [30]. FFEM has been utilized in the studies using epidermis [31] and SC [28,32,33]. The technique has been useful for studying the changes in cell membranes and barrier properties [34–36], the localization of the ultrastructure of the permeability barrier in the epidermis [29,37], the ultrastructural changes in the SC after the application of surfactants [32], liposomes [38], or iontophoresis [39], and the mode of action of skin permeation enhancers, e.g. dimethyl sulphoxide [40] and azones [40]. The combination of DTA and FFEM have been used recently to elucidate the working mechanism of azone [23].

2. Experimental

2.1. Preparation of human SC samples

Human breast or abdominal skin obtained by surgical operation was processed immediately upon arrival on the day of the surgery. After the removal of subcutaneous fat, the skin was dermatomed using an electric dermatome (Padgett Dermatome, Kansas City, USA) to a thickness of approximately 300 μm. The surface of the skin sheet was wiped clean using a tissue paper soaked with Millipore-purified water. The skin sheet was then spread, dermal side down, on a Whatman paper soaked in a 0.1% w/w Trypsin Type III (from bovine pancreas, Sigma Chemicals, St. Louis, USA) solution in 0.15 M phosphate buffered saline (PBS, pH 7.4). This buffer consisted of 0.149 M NaCl, 2 mM KH_2PO_4 and 2 mM $NaHPO_4$ in purified water. The salts used to make PBS were supplied by Merck, Darmstadt, Germany. The skin was incubated with the enzyme solution for 24 h at 4°C and then for 1 h at 37°C. Thereafter SC was carefully separated from the underlying epidermis using a pair of tweezers. Remaining trypsin activity was blocked by submerging and shaking the SC sheet in 0.1% w/w Trypsin Inhibitor Type II (from soybean, Sigma Chemicals, St. Louis, USA) solution in distilled water. Subsequently, the SC sheet was washed twice in purified water. The sheet was then dried and stored above silica gel in nitrogen atmosphere at room temperature.

2.1.1. Dehydrated

SC samples were prepared by placing SC sheets for 24 h at 50°C in a closed vessel above phosphorus pentoxide (10 mg cm^{-3} vessel volume) (JT Baker, Deventer, The Netherlands).

Table 1
Endothermic transitions of human stratum corneum

Average temperature (°C)	Assigned to	Reference
−10	lipid with low melting points	[20]
40	lateral lipid packing phase transition from orthorhombic to hexagonal	[16,46]
70	lipid structure transformation from lamellar to disordered; lateral packing to liquid	[16,17]
80	protein-associated lipid transition from gel to liquid	[6,17,18]
100	irreversible protein denaturation	[16]

2.1.2. Hydrated

SC samples were prepared by equilibrating SC sheets for 24 h at room temperature in a closed vessel above a 27% w/v sodium bromide solution in purified water. Sodium bromide was supplied by Merck, Darmstadt, Germany.

2.2. Pretreatments of SC samples

A piece of SC sheet, either dehydrated or hydrated prior to pretreatments, was submerged (without stirring) in either pure propylene glycol (PG) or 0.16 M oleic acid (OA) in PG solutions (2 ml/10 μg SC) for 24 h at 32°C. Then the SC sheet was dried by pressing it manually between 2 pieces of nylon wire-netting wrapped with tissue-paper repeatedly until the sheets did not wet the paper anymore. PG was purchased from J.T. Baker, Deventer, The Netherlands, and OA was purchased from Brocacef, Maarssen, The Netherlands.

2.3. Differential thermal analysis

SC samples (dry, prehydrated or penetration enhancer pretreated), each weighing 10–30 mg, were placed into medium pressure stainless steel crucibles made by Mettler, Greifensee, Switzerland, and hermetically sealed to avoid water evaporation during the analysis. Differential thermal analysis was performed using Mettler TA 3000 Thermal Analysis System with a Low Temperature Cell, with an empty pan as reference. Samples were subjected to the following thermal analysis cycle: cooling from 20 to −130°C, then equilibrating isothermally for at least 5 min to achieve a stable condition at −130°C, followed by heating from −130 to 120°C. The rate for both cooling and heating was 2°C min^{-1}. The transition temperatures were determined by taking the temperature corresponding to the top of peaks on the heating curves. The heating curves were constructed by plotting the heat flow values, which have been normalised using sample weight (as mW/mg), against temperatures.

2.4. Freeze fracture electron microscopy

SC sheets were cut with a razor blade into small 'ribbons' of approximately 1×8 mm. The ribbons were folded in a U-shape – anatomical surface facing outward – into cylindrical sample holders made of 83.5% silver and 16.5% copper [41]. After filling the sample holders, the samples were clamped between a pair of stainless steel tweezers and then cryo-fixed by plunging into liquid propane (−180°C) ensuring rapid freezing (10^5 K s^{-1}) of the samples without water crystallization (installation: KF80 Reichert-Jung, Vienna, Austria). The frozen samples were fixed on a specimen table and placed in the vacuum chamber of a freeze fracture device (BAF 400D, Balzers, Liechtenstein) precooled to −150°C. After the evacuation ($p<10^{-6}$ Torr) the temperature of the table was increased to −115°C and the sample was fractured by one firm forward movement of the knife of the freeze fracture device. Replicas of the fractured surface were made by deposition in unilateral direction of platinum (45°, 2.5 nm) and carbon (90°, 35 nm). The replicas were then removed from the vacuum chamber, thawed and submerged for 7 days in the cleaning reagent, 0.5 mol l^{-1} tetradecyl-dodecyl-dimethylammonium hydroxide in toluene (Soluene-350, Packard Instrument Co., Meriden, USA), for the removal of the tissue from the replica [42]. Because of the evaporation of toluene from the Soluene solution, toluene was replenished each day. After complete dissolution of all tissue material, the replicas were washed with toluene and water, respectively. Replicas were mounted on 400 mesh copper grids (Balzers, Liechtenstein). After the replicas were dried, they were examined in a transmission electron microscopy (Philips EM300, Eindhoven, The Netherlands) operated at 80 kV.

3. Results

3.1. Thermal analysis

The results of thermal analysis on SC samples with and without any pretreatments are presented in two figures: Fig. 1 pertaining to *dehydrated* SC samples and Fig. 2 concerning the *hydrated* SC samples. The endothermic transitions of untreated dry and hydrated samples, as listed in Table 1, can be recognized in the curve 1 of both figures, except for the one at 40°C which is usually very weak. The transition at −20 and 100°C are observed only in the hydrated SC (>15% water content) [19] and are assigned to water and protein, respectively [20]. The most obvious transi-

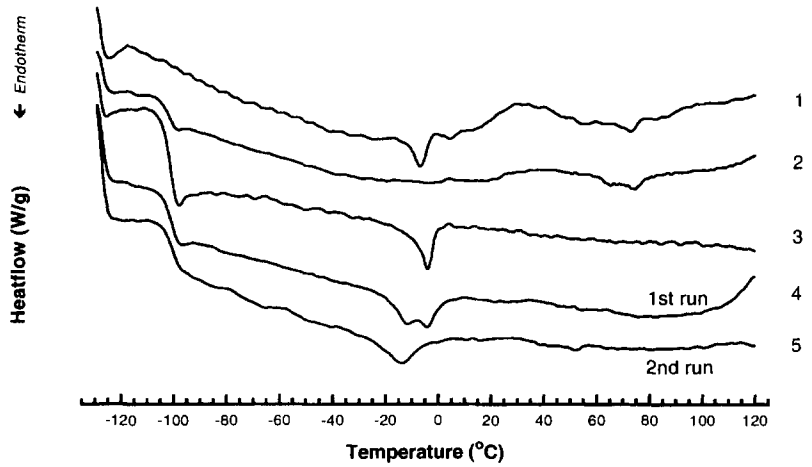

Fig. 1. Thermal profiles of (1) *dehydrated* human stratum corneum (SC) before any other treatments, and (2) after the treatment of propylene glycol; (3) 0.16 M oleic acid/propylene glycol solution (without SC); (4) *dehydrated* human SC after the treatment of 0.16 M oleic acid/propylene glycol; (5) second analysis of (4).

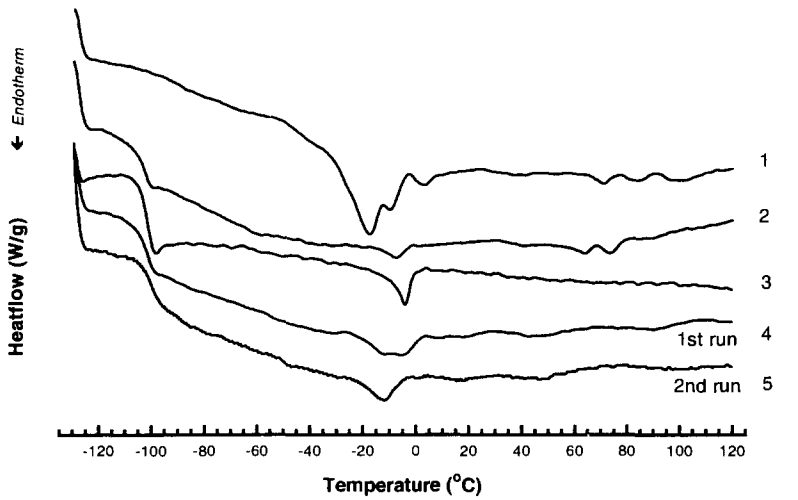

Fig. 2. Thermal profiles of (1) *hydrated* human stratum corneum (SC) before any other treatments, and (2) after the treatment of propylene glycol; (3) 0.16 M oleic acid/propylene glycol solution (without SC); (4) *hydrated* human SC after the treatment of 0.16 M oleic acid/propylene glycol; (5) second analysis of (4).

tions of these DTA scans are located at subzero temperatures, i.e. at approximately −20 and −10°C and in this study we focused on them for two reasons: (i) they belong exclusively and separately to water and lipids, hence they are convenient for interpretation, (ii) they are sensitive and indicative to enhancer effects.

3.1.1. Dehydrated human SC

The results depicted in Fig. 1 are focused on dehydrated SC samples. The subzero lipid peak at −10°C can be clearly observed in the dehydrated SC prior to any treatments (curve 1). Treatment of SC with PG reduced the enthalpy of the lipid peaks, due to a direct interaction with lipids [19], including the subzero peak

(curve 2). PG also decreased the transition temperatures at 70 and 80°C. As controls, the treatment solutions alone were analyzed separately. Pure PG exerted only one transition at −100°C (data not shown), while OA/PG exerted two transitions at −100 and −5°C (curve 3). The last transition belongs exclusively to OA. Thermal analysis of dehydrated SC samples treated with OA/PG resulted in curve 4. The transitions in the temperature region above 0°C almost completely disappeared indicating a strong decrease in enthalpy. The subzero peaks can still be observed. Three transitions are noticed in this region: at −5, −12 and −100°C. The transition peaks at −5 and −100°C can be assigned to OA/PG (cf. curve 3). The transition at −12°C, however, is new. This peak is apparently a result of the shift in the subzero lipid transition at −10°C due to interactions between the SC lipids and the OA solution. When the same sample was heated to 120°C, cooled down and subsequently analyzed again from −130 to 120°C (referred to in Fig. 1 as the second analysis), both peaks at −5 and −12°C disappeared and a single peak at −13°C appeared (curve 5). The second analyses performed either on the same day or after 14 days gave comparable results. The unification of the two transitions into one implies that a mixing process of the two components – SC lipids and OA – occurred with the aid of heating.

3.1.2. *Hydrated human SC*

The thermoscans pertaining to hydrated SC samples (containing 20% weight of water) are collected in Fig. 2. The first curve is assessed from a sample prior to any other pretreatments. In the subzero region, a large peak at −20°C, assigned to water, is immediately noticeable. A subzero lipid transition at −10°C can still be recognized, partially or completely covered by the water peak. The treatment of PG to this type of sample annihilated the water peak, leaving the transition at −10°C clearly visible (curve 2). Furthermore,

Fig. 3. Freeze fracture electron micrograph of *hydrated* human SC before any other pre-treatments. Legend for freeze fracture electron micrograph: Scale bar indicates 1 μm; Arrow indicates the direction of Pt shadowing. C: corneocyte; L: lipid lamellae; S: smooth granular region; R: rough granular region.

the transition temperatures at 70 and 80°C were decreased, accompanied by a less pronounced change in enthalpy compared to the corresponding scan in Fig. 1. Identical to what is already shown in the previous section, OA/PG yielded transitions at −5 and −100°C, of which the peak at −5°C is due to the presence of OA (curve 3). On the other hand, the transitions in the temperature region above 0°C almost completely disappeared. The analysis of the hydrated SC treated with OA/PG resulted in curve 4, in which the peaks at −5 and −12°C were almost identical to those of dehydrated samples observed on the corresponding curve 4 in Fig. 1. In the presence of PG, the degree of hydration obviously does not play any role to the thermal behaviour of SC. The reheating of the same sample yielded curve 5 with a single peak at −13°C, instead of two peaks at −5 and −12°C, very similar to the corresponding curve 5 in Fig. 1. Again, this implies strongly that the two components have a tendency to mix with each other at elevated temperatures.

3.2. *Freeze fracture electron microscopy*

The freeze fracture electron micrograph in Fig. 3 shows hydrated human SC without any pre-treatments. SC is composed of granular corneocytes embedded in a matrix of intercellular lipid. As characterized in Van Hal et al. [33], in fully hydrated SC, the intercellular lipid region consists mainly of bilayers or lamellae forming regions having either smooth or rougher surfaces. It also contains desmosomes, extrusions and several other formations, which can sporadically be observed in some samples. This picture does not show any significant differences in the ultrastructures of SC compared to those after the pre-treatment of PG (see Fig. 4) either on the dehydrated or hydrated SC. The only exception is the appearance of PG with typical isotropic, granular fracturing pattern surrounding the corneocytes, as described by Hoogstraate et al. [43]. However, after the application of OA in PG solution, the electron micrograph in Fig. 5 revealed the existence of 3

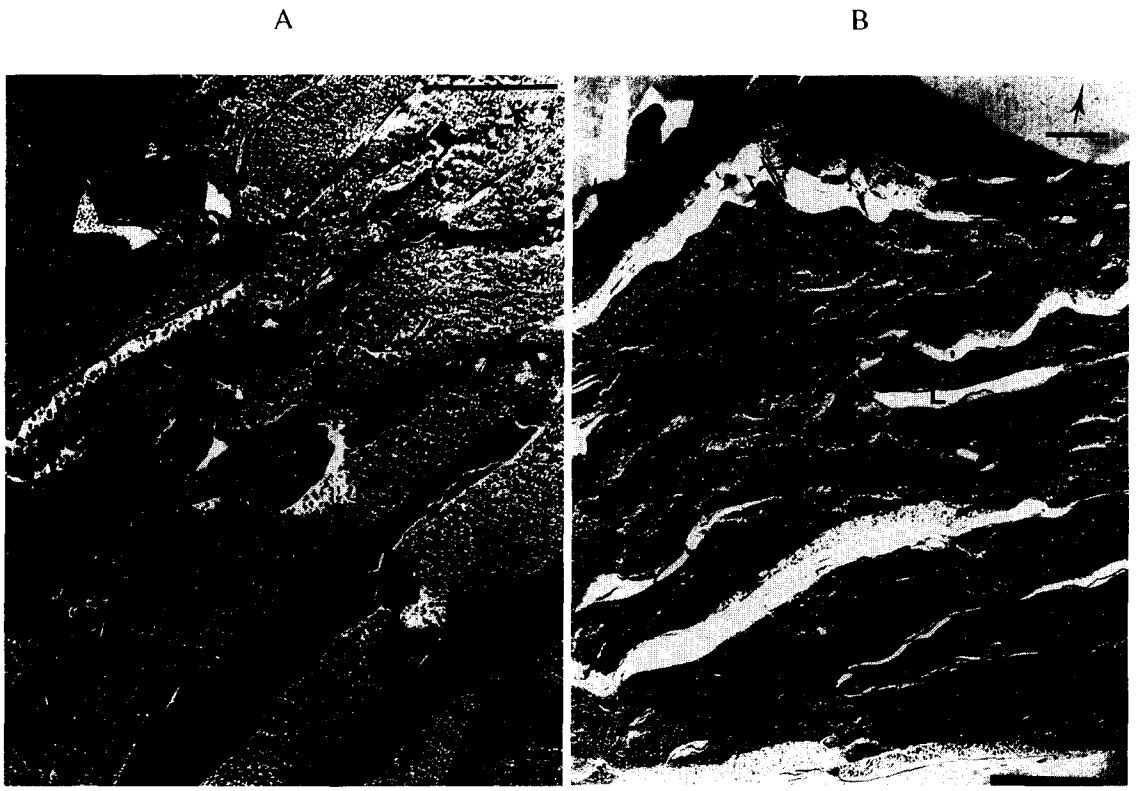

Fig. 4. Freeze fracture electron micrograph of (A) *dehydrated* and (B) *hydrated* human SC after the pre-treatment of propylene glycol.

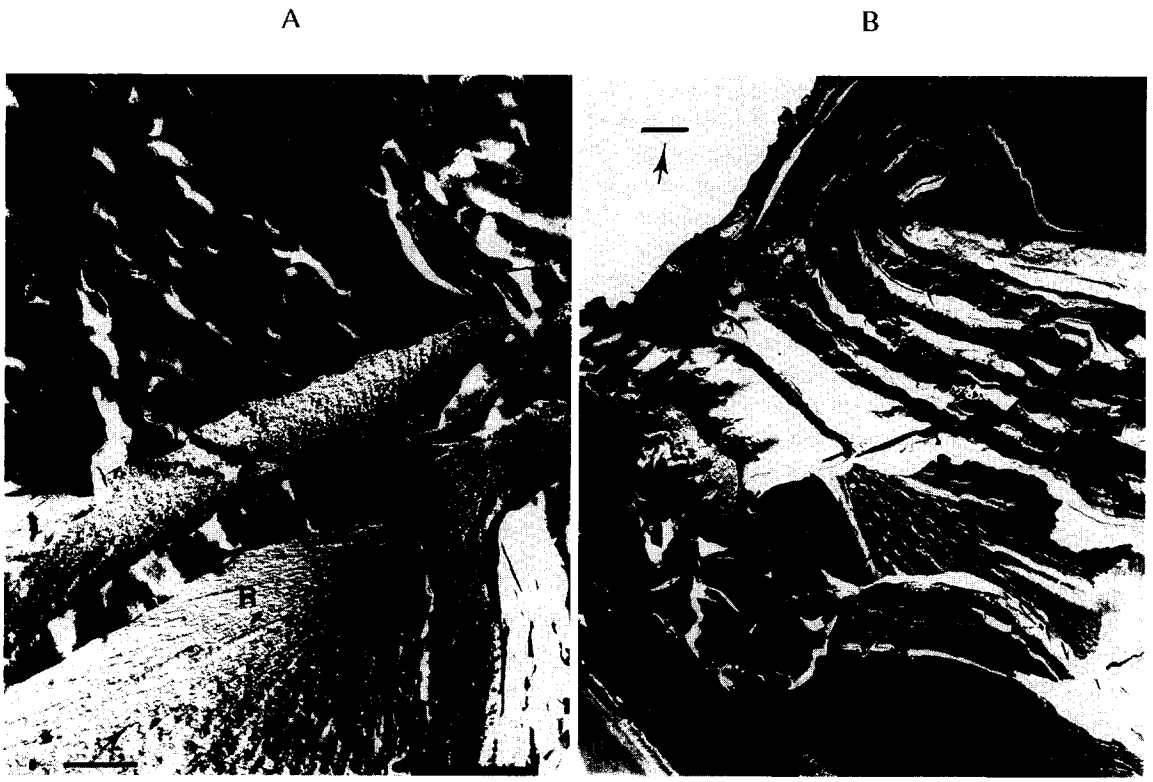

Fig. 5. Freeze fracture electron micrograph of (A) *dehydrated* and (B) *hydrated* human SC after the pre-treatment of 0.16 M oleic acid in propylene glycol.

types of structures in the SC lipid domain: (i) regions showing lamellar structures observable in the untreated samples, observed in a few samples, (ii) smooth, fine granular regions, and (iii) rough, scaly regions, which did not appear in the previously mentioned electron micrographs (of untreated or PG treated SC). The smooth, isotropic regions with fine granulars are primarily observed at the outer surfaces of the samples, suggesting its origin to be the native OA/PG solution. Similar regions within the SC indicate that OA/PG may exist in the SC intercellular space in separate domains. The rough scally structure, however, cannot be contributed to either OA/PG or the normally observed intercellular lamellae. This is a strong indication that OA, PG and skin lipids in the intercellular region form a mixture with a new type of ultrastructure. The appearance of the rough structure has also been observed in the study using azones [23].

4. Discussion

Following the pretreatment of SC with PG alone, the significant effects observed in the thermoscans are concerning water and protein. However, less but clear effects were also noticed on the lipids in the form of decreased transition temperatures at 70 and 80°C accompanied by slight decrease in enthalpy. These transitions, particularly the one at 80°C, have been associated with proteins, probably in the form of a lipid–protein complex [17–19]. This association may mainly exist at the border between corneocyte and the intercellular lipid. In the electron micrographs, PG has been found primarily surrounding the corneocytes. It cannot, however, be excluded that a portion of PG does penetrate into the cells or into the intercellular lipid bilayers, knowing that PG has a high molecular mobility and a broad compatibility with proteins and lipids [44]. It can be suggested that the disruption of the

lipid–protein interaction at the cell-envelope region is the mode of action of PG on SC. From the cell membrane, PG may withdraw water from the protein in the cell owing to its hygroscopicity causing the vanishing of the thermal denaturation peak at −100°C (on hydrated samples). The loss of interaction with protein may decrease the transition temperatures of the lipids (at 70 and 80°C), since less energy will be required for gel–liquid transformation without the necessity to break the lipid–protein bonding.

Thermal analysis of SC pre-treated with OA indicates an interaction between the acid and skin lipids. OA has been known to partially solubilize SC lipids, particularly observed from the reduction in the enthalpies of endothermic lipid transitions located between 60 and 90°C [6]. The degree of enthalpy reduction is apparently dependent on the duration of the treatment. A short term treatment (30 s to 1 h) performed by Goodman and Barry [6] resulted in approximately 50% decrease in enthalpy, whereas a 24 h treatment in the present study almost completely reduced the transitions. This indicates a gradual, slow change as a result of the OA/PG treatment. The subzero skin lipid transition peak and the peak of OA (in PG solution) fused together forming one single peak at a lower temperature than those of the components. It was suggested previously [20] that this interaction may well be based on the formation of a eutectic mixture between oleic acid and skin lipids as often occurs in multicomponent lipid mixtures, for instance the binary system of fatty acids [45]. This phenomenon was clearly observed only after reheating, but it cannot be ruled out that the mixing process has been taking place since the beginning of the application. The evidence is the shift of the subzero skin lipid transition (−10°C) to −12°C observed in the samples analyzed directly after the removal of the application. In the analysis of such samples, both the transition of native OA and the transition of OA–skin lipid mixture were present. This fact gives an indication that OA may perturb stratum corneum lipids functioning as the skin barrier by both forming separate OA-rich domains in the SC intercellular lipid region and forming a eutectic mixture with endogenous skin lipid components with a lower melting point. In both cases the integrity of the skin barrier function is so perturbed that its permeability toward many permeants increases.

After the same treatment of OA/PG as in the thermal analysis, three distinctive ultrastructures can be observed from the electron micrographs: (i) smooth, isotropic, fine granular regions, (ii) the lamellar structure normally found in the untreated SC, and (iii) rough granular region. The appearance of these structures can be correlated with three major transitions observed in the corresponding thermal analysis curve: at −100, −12 and −5°C, respectively. As the smooth region can be assigned to PG-rich region, it may have a transition at −100°C, which is characteristic for pure PG. The OA–skin lipids mixture may exist in the OA-rich domains and skin lipids-rich domains which exert the transitions at −5 and −12°C, respectively. We speculate that the normally looking lipid lamellae regions are the skin lipids-rich domain, while the rough granular regions comprise of the separated OA-rich domains.

5. Conclusion

The results of the present study bring up a perspective on the mode of action of OA in perturbing the skin barrier function, i.e. by both *eutectic mixing* with skin lipids and *forming separate OA-rich domains*. Either the newly formed lipid mixture or excess OA accumulation or both simultaneously may play an important role in reducing the barrier capacity in comparison to untreated skin.

References

[1] A.M. Kligman, in W. Montagna and W.C.J. Lobitz (Eds.), The Epidermis, Academic Press, New York (1964) p. 387, Chap. 20.
[2] R.J. Scheuplein and I.H. Blank, Physiol. Rev., 51 (1971) 702.
[3] M.L. Francoeur, G.M. Golden and R.O. Potts, Pharm. Res., 7 (1990) 621.
[4] B.J. Aungst, in E.W. Smith and H.I. Maibach (Eds.), Percutaneous Penetration Enhancers, CRC Press, Boca Raton (1995) p. 277, Chap. 9.1.
[5] B.J. Aungst, J.A. Blake and M.A. Hussain, Pharm. Res., 7 (1990) 712.
[6] M. Goodman and B.W. Barry, in R.L. Bronaugh and H.I. Maibach (Eds.), Percutaneous Absorption, Marcel Dekker, New York, 2nd edn. (1989) p. 567.
[7] R.H. Guy, V.H.W. Mak, T. Kai, D. Bommannan and R.O. Potts, in R.C. Scott and R.H. Guy (Eds.), Prediction of

Percutaneous Penetration – Methods, Measurements, Modelling, IBC Technical Services, London (1990) p. 213.
[8] C.L. Gay, J. Hadgraft, I.W. Kellaway, J.C. Evans and C.C. Rowlands, in R.C. Scott and R.H. Guy (Eds.), Prediction of Percutaneous Penetration – Methods, Measurements, Modelling, IBC Technical Services, London (1990) p. 322.
[9] B. Ongpipattanakul, R.R. Burnette, R.O. Potts and M.L. Francoeur, Pharm. Res., 8 (1991) 350.
[10] M. Walker and J. Hadgraft, Int. J. Pharm., 71 (1991) R1.
[11] B. Forslind, Acta Derm. Venereol. (Stockh.), 74 (1994) 1.
[12] A. Naik, L.A.R.M. Pechtold, R.O. Potts and R.H. Guy, J. Controlled Rel., 37 (1995) 299.
[13] J.J. Bulgin and L.J. Vinson, Biochim. Biophys. Acta, 136 (1967) 551.
[14] K. Walkley, J. Invest. Dermatol., 59 (1972) 225.
[15] G. Imokawa, H. Kuno and M. Kawai, J. Invest. Dermatol., 96 (1991) 845.
[16] B.F. van Duzee, J. Invest. Dermatol., 65 (1975) 404.
[17] K. Knutson, R.O. Potts, D.B. Guzek, G.M. Golden, J.E. McKie, W.J. Lambert and W.I. Higuchi, J. Controlled Rel., 2 (1985) 67.
[18] G.M. Golden, D.B. Guzek, R.R. Harris, J.E. McKie and R.O. Potts, J. Invest. Dermatol., 86 (1986) 255.
[19] J.A. Bouwstra, M.A. de Vries, G.S. Gooris, W. Bras, J. Brussee and M. Ponec, J. Controlled Rel., 15 (1991) 209.
[20] H. Tanojo, J.A. Bouwstra, H.E. Junginger and H.E. Boddé, Pharm. Res., 11 (1994) 1610.
[21] M. Goodman and B.W. Barry, Anal. Proc., 23 (1986) 397.
[22] J.A. Bouwstra, L.J.C. Peschier, J. Brussee and H.E. Boddé, Int. J. Pharm., 52 (1989) 47.
[23] H.E. Boddé, M. Ponec, A.P. IJzerman, A.J. Hoogstraate, M.A.I. Salomons-de Vries and J.A. Bouwstra, in K.A. Walters and J. Hadgraft (Eds.), Pharmaceutical Skin Penetration Enhancement, Marcel Dekker, New York (1993) p. 199, Chap. 8.
[24] J. Hirvonen, R. Rajala, P. Vihervaara, E. Laine, P. Paronen and A. Urtti, Eur. J. Pharm. Biopharm., 40 (1994) 81.
[25] P.A. Cornwell and B.W. Barry, in R.C. Scott, R.H. Guy, J. Hadgraft and H.E. Boddé (Eds.), Prediction of Percutaneous Penetration, Vol. 2, IBC Technical Services, London (1991) p. 394.
[26] B.W. Barry and A.C. Williams, in K.A. Walters and J. Hadgraft (Eds.), Pharmaceutical Skin Penetration Enhancement, Marcel Dekker, New York (1993) p. 95, Chap. 4.
[27] P. Ashton, K.A. Walters, K.R. Brain and J. Hadgraft, Int. J. Pharm., 87 (1992) 265.
[28] A.S. Breathnach, T. Goodman, C. Stolinski and M. Gross, J. Anat., 114 (1973) 65.
[29] P.M. Elias and D.S. Friend, J. Cell Biol., 65 (1975) 180.
[30] P.M. Elias, R. Orozco-Topete, M.A. Lampe, M.K. Nemanic, S. Grayson, M.L. Williams and B.E. Brown, in D. Skerrow and C.J. Skerrow (Eds.), Methods in Skin Research, John Wiley and Sons Ltd, New York (1985) p. 381, Chap. 14.
[31] H.E. Boddé, B.P. Holman, F. Spies, A. Weerheim, J. Kempenaar, M. Mommaas and M. Ponec, J. Invest. Dermatol., 95 (1990) 108.
[32] H.E.J. Hofland, J.A. Bouwstra, M. Ponec, H.E. Boddé, F. Spies, J.C. Verhoef and H.E. Junginger, J. Controlled Rel., 16 (1991) 155.
[33] D.A. van Hal, E. Jeremiasse, H.E. Junginger, F. Spies and J.A. Bouwstra, J. Invest. Dermatol., 1996 (1996) 89.
[34] P.M. Elias, D.S. Friend and J. Goerke, J. Histochem. Cytochem., 27 (1979) 1247.
[35] L. Landmann, J. Invest. Dermatol., 87 (1986) 202.
[36] M. Aszterbaum, G.K. Menon, K.R. Feingold and M.L. Williams, Pediatr. Res., 31 (1992) 308.
[37] P.M. Elias, J. Goerke and D.S. Friend, J. Invest. Dermatol., 69 (1977) 535.
[38] H.E.J. Hofland, J.A. Bouwstra, H.E. Boddé, F. Spies and H.E. Junginger, Br. J. Dermatol., 132 (1995) 853.
[39] W.H.M. Craane-van Hinsberg (1994) Transdermal peptide iontophoresis: a mechanistic study of electrical skin barrier perturbation and transport enhancement. Ph.D. Thesis, Rijksuniversiteit, Leiden.
[40] H.E. Boddé, M.A.M. Kruithof, J. Brussee and H.K. Koerten, Int. J. Pharm., 53 (1989) 13.
[41] B.P. Holman, F. Spies and H.E. Boddé, J. Invest. Dermatol., 94 (1990) 332.
[42] F. Spies, H.E. Boddé, H.E.J. Hofland and J.M. Van't Noordende (1992) personal communication. Quoted in: H.E.J. Hofland, J.A. Bouwstra, H.E. Boddé, F. Spies, H.E. Junginger, Br. J. Dermatol., 132 (1995) 853.
[43] A.J. Hoogstraate, J. Verhoef, J. Brusee, A.P. IJzerman, F. Spies and H.E. Boddé, Int. J. Pharm., 76 (1991) 37.
[44] J.A. Bouwstra, M.A. Salomons-de Vries, B.A.I. van den Bergh, J. Brussee and G.S. Gooris, Int. J. Pharm., in press.
[45] E.S. Lutton, in K.S. Markley (Ed.), Fatty acids, Interscience, New York (1967) p. 2583, Chap. 22. Part 4.
[46] G.L. Wilkes, A.L. Nguyen and R.H. Wildnauer, Biochim. Biophys. Acta, 304 (1973) 267.